Integrated multi-objective optimisation of the support structure of heliostats in concentrated solar power plants using a genetic algorithm

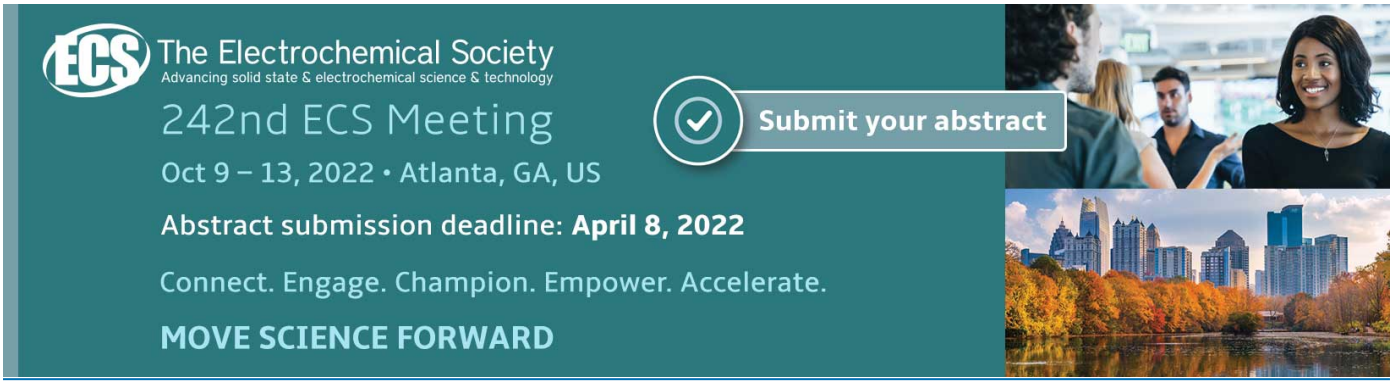

Integrated multi-objective optimisation of the support structure of heliostats in concentrated solar power plants using a genetic algorithm

L Lomazzi[1], F Cadini[1]*, M Giglio[1], C Cancro[2], G Ciniglio[2], G Graditi[2] and A Pontecorvo[2]

[1]Politecnico di Milano, Department of Mechanical Engineering, Via La Masa n.1, Milan, Italy
[2] Italian National Agency for New Technologies, Energy and Sustainable Economic Development, ENEA – Research Center, Piazza E. Fermi 1, 80055, Portici (NA), Italy

*Corresponding author: francesco.cadini@polimi.it

Abstract. The optimisation of the support structure of heliostats in concentrating solar power plants is a fundamental task aimed at attempting to reduce the high levelised cost of energy (LCOE) of current configurations. In this work, an integrated multi-objective optimisation framework is presented, which relies on the combination of a lean and fast structural model with a genetic algorithm to simultaneously minimise both the overall mass of the support structure and the mean angle of rotation of the mirror surface, which directly affects the optical efficiency of the component. A particular feature of the proposed framework is that it represents an integrated solution, i.e., it allows to simultaneously optimise the main components of the heliostat support structure, i.e., the pedestal, the truss and the back support structure, assuming they are off-the-shelf components easily available on the market. The optimisation problem is set up selecting as design variables (i) the number of elements in the back support structure and (ii) the relevant characteristics of all the components considered, i.e., section shape and dimensions, according to the components commercial datasheets. At each iteration of the optimisation process, the structural model is fed with the current design variables values and, according to some computed aerodynamic loads, it allows evaluating the displacement and rotation of the points of interest within the mirror surface. An aerodynamic model present in the literature based on experimental wind tunnel tests is used to estimate the wind forces acting on the heliostat as a function both of the mirror inclination angle with respect to the ground and of the wind direction with respect to the mirror orientation. In this work, the proposed methodology is demonstrated on a realistic case study and the results commented in detail, highlighting possible future developments and the limitations of the framework.

1. Introduction

The cost of heliostats is an impacting factor on the overall cost of concentrated solar power plants [1]. Since most of this cost is determined by the amount of material of the heliostat support structure, driving the design phase of such a structure towards weight reduction would be beneficial to reduce the high levelised cost of energy (LCOE) of current configurations [2]. Several studies have been

conducted in the past years on possible cost reduction strategies, these have identified that both the heliostat size and the properties of the elements in the support structure should be optimised to achieve an effective cost reduction [3–6]. However, the selection of the structural designs should not only rely on the cost of the structure, but also on its performance. In fact, lean heliostat supports may lead to cheap structures, while allowing for deformations under operative loads, such as wind loading and gravity, that may result in unsatisfactory optical efficiency [7]. Hence, the heliostat structural design should pursue a trade-off between the cost of the system and its performance. To this purpose, it is paramount to determine the structural deformation of the reflective surface of the heliostat, which is herein referred to as *mirror*, under gravity and wind loading, since it directly affects the optical efficiency of the system [8]. The mechanical performance of the heliostat structure under the loading conditions mentioned above is typically assessed resorting to finite element analyses [9–11]. However, this type of analysis is computationally demanding and is not compatible with an efficient structural design optimisation scheme, which would benefit from faster methods to evaluate the mechanical performance of possible structures. Despite this, some works in the literature have been proposed that optimise the heliostat structure employing finite element models to evaluate the mechanical performance of the design, but the optimisation approach is limited to the evaluation of a little number of possible solutions [2,6]. Instead, an optimisation approach that evaluates a satisfactory number of possible solutions is presented in the work in [12], that employs a particle swarm optimisation algorithm to identify the best heliostat shape that simultaneously minimises the occupied field area and maximises the field efficiency. However, to the authors' best knowledge, extensive approaches of this type focused on the structural optimisation of the heliostat structure appear to be missing in the literature.

In this work, a methodological approach to the optimisation of the support structure of heliostats in concentrated solar power plants is presented. The proposed methodology relies on an optimisation framework based on a genetic algorithm, that interacts with a simplified structural model of the heliostat structure to drive the design process towards the simultaneous minimisation of the structural weight and of the mirror mean deformation. This paper is organised as follows. Section 2 presents the main features of the structural model and of the optimisation framework proposed in this work. Section 3 demonstrates the approach to the optimal design of the heliostat support structure by means of a realistic case study and discusses the main results of the optimisation process. Finally, Section 4 draws out the conclusions from this work.

2. Methodological approach

In this Section the methodological approach set up to identify the optimal configuration of the support structure of heliostats in concentrated solar power plants is presented. This approach involves the interaction between the structural model of the heliostat support structure and the optimisation method employed, which is identified in a genetic algorithm.

2.1. Structural model of the heliostat support structure

The heliostat structure considered in this work is shown in Figure 1.

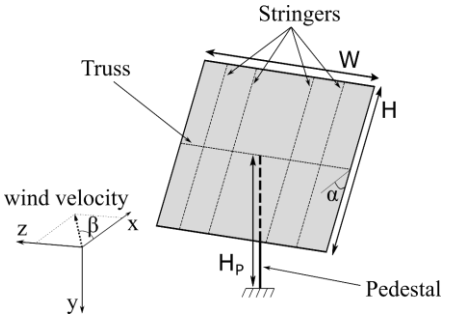

Figure 1. Heliostat considered in this work.

The heliostat structure is composed of the mirror and its support structure, that includes the stringers, the truss and the pedestal. The mirror stiffness is neglected in the computations, while all the structural components of the support structure are simplified as beams clamped at the mutual intersections. Hence, the pedestal is composed of one single element from the ground to the truss, the truss is assumed to be clamped at its geometrical centre, in correspondence of the intersection with the pedestal, while one end of each stringer is considered to be clamped at the intersection with the truss. Geometric symmetry is exploited to speed up the computations. In fact, since the structure is symmetric with respect to the planes perpendicular to the mirror surface passing through the edges mid points, structural evaluations are performed considering one quarter of the support structure only, retrieving the results at the other quarters thanks to symmetry considerations. This is shown in Figure 2, where the mirror symmetry planes are identified and the quarter selected for the computations is highlighted with black diagonal stripes.

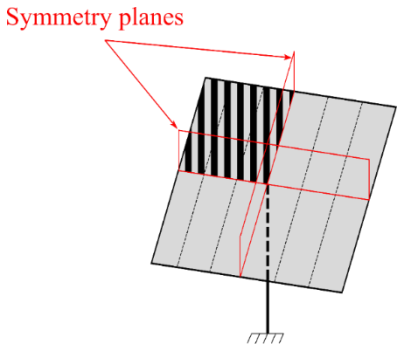

Figure 2. Symmetry planes and quarter selected for the computations (black diagonal stripes).

The structural computations are performed resorting to the Euler-Bernoulli beam theory [13]. The main assumption of the structural model is that all the loads acting on the structural elements in a position different from the beam ends are simplified as distributed equivalent loads acting over the whole length of the element. The authors verified that this assumption is reasonable and does not limit the validity of the approach, but this proof is not reported here for the sake of brevity. Moreover, all the structural elements are assumed to be described by a perfectly linear material constitutive law. This assumption allows determining the deflection and the rotation of some points of interest along the structural elements, independently considering each structural element, linearly combining these results in a later phase of the computations to get the overall displacement of the points of interest on the mirror surface.

The loading condition is represented by (i) the weight of the structural elements and of the mirror and (ii) wind forces and moments acting along the axes of the reference system shown in Figure 1. In particular, according to the considerations in the work in [14], only the aerodynamic forces along the x and the y axes and the aerodynamic moments described by vectors directed as the y and the z axes, i.e., the azimuth and elevation moments, respectively, are considered in the structural model. The magnitude of the wind loads is computed according to the equations presented in the work in [14], which are not reported here for the sake of brevity. The user-defined parameters representing the input values to the aerodynamic equations are the wind direction, which lies in the xz plane and is identified by the azimuth angle (β), i.e., the horizontal misalignment between the wind direction and the vector normal to the mirror surface, and the mirror elevation angle (α) (Figure 1), the wind peak velocity ($V_{w,p}$), the wind peak velocity-to-mean velocity ratio (r), the height of the wind velocity measuring station (H_w) and an adimensional number accounting for environmental effects (n).

No more information is reported in this Section about the structural model, since this is not the main focus of this work and since the equations employed, e.g., the Euler-Bernoulli beam theory equations, are well known to the research community.

2.2. Optimisation method

The optimisation method employed in this work involves a genetic algorithm. This type of algorithms is commonly used in several engineering fields to identify minima and maxima of a function of interest. In particular, with regards to structural engineering applications, this method is typically employed to optimise the structural design in terms of minimisation of the weight of the solution and maximisation of its stiffness.

In this context, embedding optimisation procedures into the design process of the heliostat structure represents a promising approach to identify the optimal structural configurations. In this work, the optimal configurations are represented by the set of structural solutions that simultaneously minimise both the weight of the support structure of the mirror and its average deformation.

With regards to the structural configuration described in Section 2.1, the design variables considered in the optimisation process are represented by (i) the number of stringers (x_1), (ii) the stringers section properties (x_2), (iii) the truss section properties (x_3) and (iv) the pedestal section properties (x_4). The design variables are all described by discrete integer numbers only. In fact, the design variables representing the section properties are identified by the corresponding index within a built-in database of off-the-shelf components easily available on the market including H, T, hollow rectangular, hollow square and hollow circular-shaped sections [15]. Two objective functions are considered in the optimisation process, i.e., the weight of the structural support structure (W) and the mean deformation of the mirror (R). The latter is included in the analysis since minimising the mirror deformation is equivalent to maximising the optical efficiency of the heliostat, which represents a paramount variable for this type of systems. Note that in this work *deformation* refers to the mirror rotation vector component lying in the mirror plane, which is computed as the mean value of the deformation measured at some points of interest within the mirror surface. Hence, identifying with α the elevation angle of the mirror (**Figure 1**) and with *i* the *i*th point of interest within the mirror surface, the objective functions considered in this work are defined by Equations (1) and (2):

$$W=W_{stringers}+W_{truss}+W_{pedestal} \tag{1}$$

$$R=\text{mean}\left(rot^{\alpha}_{//,i}\right) \quad \forall\alpha,i \tag{2}$$

where $W_{stringers}$, W_{truss} and $W_{pedestal}$ are the stringers, the truss and the pedestal weight values, respectively, while $rot^{\alpha}_{//,i}$ represents the rotation of the *i*th point of interest when the mirror is characterised by the elevation angle α. Note that the optimisation process considered in this work is a multi-objective optimisation process, since two objective functions are involved to evaluate the possible solutions.

More details on the specific parameters of the genetic algorithm employed in the optimisation framework are presented in the case study shown in Section 3.

3. Case Study

In this Section the proposed methodology is demonstrated by means of a case study.

The heliostat considered in this case study is shown in Figure 3. It consists of a 5mm thick mirror with surface size 6x6m^2 and density ρ_m=2.5kg/m^2 mm, backed by a support structure composed of stringers, one truss and one 3.4m high pedestal. The structural elements of the support structure are made of a generic steel with density ρ_s=7890kg/m^3, Elastic modulus E=200GPa, Poisson's ratio ν=0.33 and yield stress σ_{VM}=355MPa.

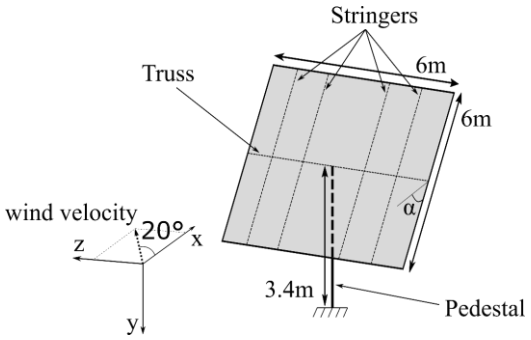

Figure 3. Heliostat structure considered in the case study.

Three elevation angles are considered in the analysis, i.e., α=[30°,50°,70°], and the wind velocity is assumed to hit the mirror with azimuth angle β=20° to consider the most critical wind loading conditions [14]. Moreover, the heliostat is supposed to be placed in free field (n=0.143 [14]) and to be hit by wind with peak velocity $V_{w,p}$=64km/h and peak velocity-to-mean velocity ratio equal to r=1.6. The wind data are assumed to have been obtained from a H_w=4m high measuring station.

As already anticipated in Section 2.2, the design variables are identified in (i) the number of stringers (x_1), (ii) the stringers section properties (x_2), (iii) the truss section properties (x_3) and (iv) the pedestal section properties (x_4). Some constraints are introduced in the analysis to limit the range of variability of the design variables. In particular, x_1 can only assume integer numbers from 2 to 8, the stringers and the truss sections can vary within the whole database, which is composed of 213 structural solutions, while the pedestal is limited to hollow rectangular, square and circular-shaped sections. For the sake of clarity, the index ranges identifying the different section shapes in the database considered in this work are shown in Table 1.

Table 1. Database composition.

Section shape	Index range
H	[1, 18]
T	[19, 29]
Hollow rectangular	[30, 116]
Hollow square	[117, 164]
Hollow circular	[165, 213]

The optimisation process is set up using the Matlab® algorithm *gamultiobj*, which is a genetic algorithm specifically implemented for multi-objective problems [16]. Note that, being this case study a multi-objective problem, a set of optimal solutions will be identified by the optimisation process, i.e., those solutions lying on the Pareto front of the problem. The initial population size is set to $N_P = 100$ individuals and is randomly generated. This number of individuals is identified as a satisfactory trade-off between computational resources required and discretisation of the Pareto front. In fact, considering a larger population would on the one hand increase the time required to evaluate the objective functions of the whole population, while on the other hand it would allow describing the numerical Pareto front with more solutions, thus increasing the accuracy of the results. Moreover, a population composed of $N_P = 100$ individuals meets the requirements of the specific genetic algorithm employed in this work [16]. The default functions governing the crossover and mutation processes need to be specialised to the case of discrete integer design variables. No further information is reported in this work regarding this coding task, since this is not considered to bring any additional insight into the proposed framework. Two stop criteria are selected, i.e., maximum number of

generations $N_G = 200$ and FunctionTolerance=10^{-5} over the last $N_S = 100$ generations. The former criterion is employed to limit the required computational resources to carry out this case study, while the latter criterion is employed to stop the optimisation process whenever, simultaneously, (i) the geometric mean of the relative variation of the dispersion over the last N_S generations is lower than the FunctionTolerance value and (ii) the final dispersion value is lower than the mean dispersion value computed over the last N_S generations, where the *dispersion* is a metric measuring the movement of the set of points on the Pareto front. No more information is reported on this metrics, the interested reader is referred to [17] to go deeper into the topic.

During the optimisation process, the solver calls the structural model described in Section 2.1 to evaluate the objective functions for each individual in the current population. In particular, the genes of each individual, i.e., the design variables values, are passed to the structural model, that returns the support structure weight and the mean deformation of the mirror surface. Twelve points are selected as points of interest over which to compute the mean deformation of the mirror surface, as shown in Figure 4.

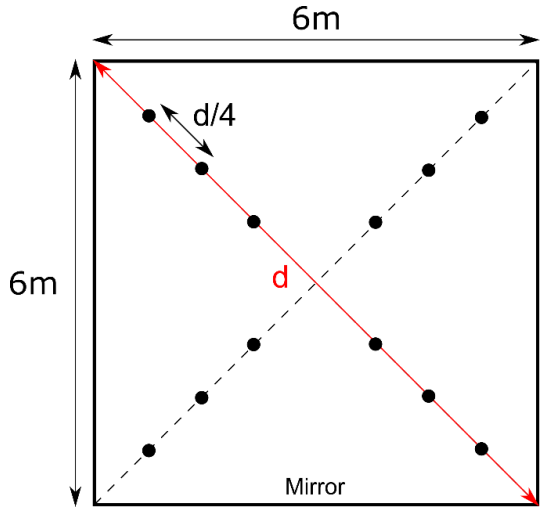

Figure 4. Points of interest on the mirror surface (black dots).

Since the structural model is implemented in the Excel software package, while the optimiser is coded in the MATLAB® environment, an interface between the two models needs to be developed. The most promising solution in terms of computational time for the analysis is identified in modelling the interface using ActiveX controls. This approach consists of creating a Microsoft server in the MATLAB® environment that allows the optimiser to directly work on the excel model, thus avoiding eventual overheads caused by the employment of the MATLAB® built-in functions *xlsread* and *xlswrite*. The adopted solution allows evaluating the objective functions of a single individual in a time $t_{ActiveX}$=2.5s, while using the built-in functions mentioned in the latter solution would require $t_{xlsread,xlswrite}$=5.6s for the same task.

With regards to this case study, the optimisation process runs for 102 generations, before stopping due to the FunctionTolerance stop criterion. The population at the last generation is reported in Figure 5.

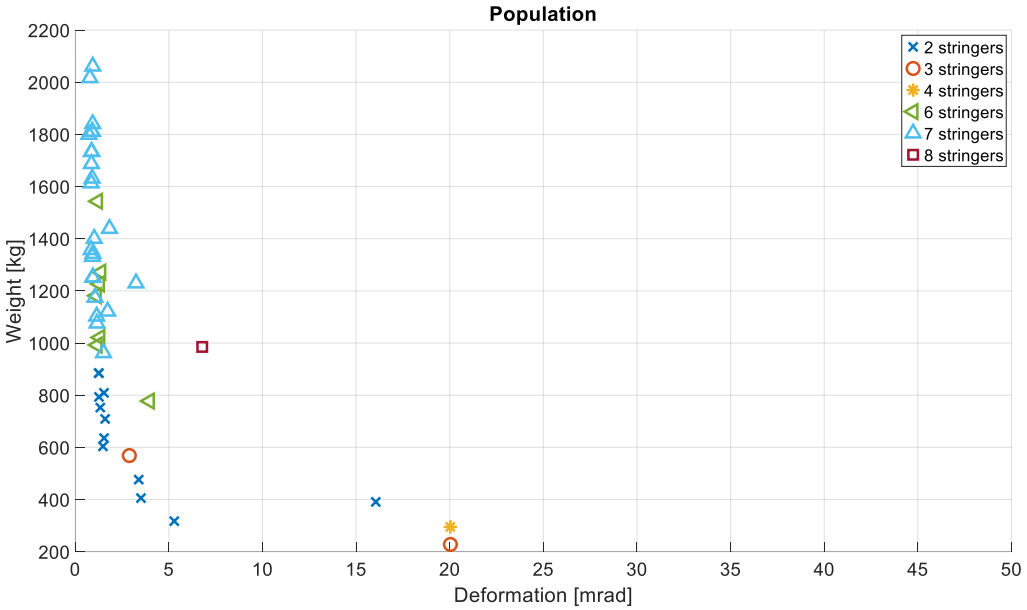

Figure 5. Population at the last generation.

The individuals shown in Figure 5 appear to be satisfactorily distributed around a hyperbolic curve limiting the optimal solutions. This hyperbolic curve represents the numerically reconstructed Pareto front and is composed of those points that represent an optimal trade-off between the objective functions, meaning that it is not possible to move from one point in the Pareto front to any other point by improving both the objective functions simultaneously. The numerical Pareto front reconstructed during the optimisation process is shown in Figure 6.

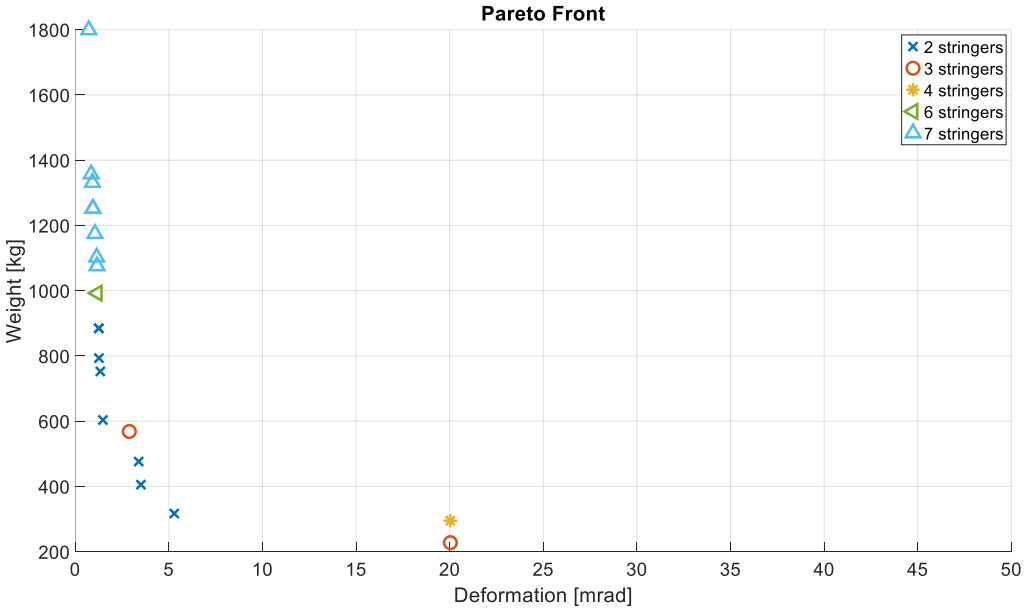

Figure 6. Numerically reconstructed Pareto front.

It is worth noting that no optimal solution with five or eight stringers, i.e., no solution with $x_1 = 5$ or $x_1 = 8$, is included in the Pareto front. This may be surprising at first sight, since the exact Pareto

front would in principle be composed of solutions with any possible value of the first design variable. In fact, keeping the sections shapes for the stringers, the truss and the pedestal constant, increasing the number of stringers would reduce the mirror deformation and increase the structural weight of the solution, thus identifying a new point in the Pareto front, according to the definition reported above. However, in this case study a limited number of individuals in the population is considered, i.e., $N_P = 100$, which does not allow having a numerically reconstructed Pareto front discretised enough to include solutions with $x_1 = 5$ or $x_1 = 8$. Despite this, the composition of the Pareto front is physically sound, since the general trend appears to satisfy the intuition that increasing the number of stringers leads to moving from solutions characterised by larger deformation and smaller weight to those with smaller deformation and larger weight. Few exceptions to this rule are present in Figure 6, but no further investigation on the causes of these exceptions is reported here because out of the scope of this work.

More information can be given regarding each identified optimal solution by further post-processing the results. In particular, a safety factor (η) can be defined to identify those structural configurations that can safely carry the wind and weight loads without the plasticisation of any of the components they are composed of. The safety factor η_j of the *j*th component of the support structure is computed according to Equation (3):

$$\eta_j = \frac{\sigma_{y,j}}{\sigma_{VM,j}} \tag{3}$$

where $\sigma_{y,j}$ and $\sigma_{VM,j}$ are the yielding stress and the Von-Mises stress of the *j*th component, respectively. Note that the term "component" is generically adopted to refer to the stringers, the truss and the pedestal. The structural solution can withstand the loads without undergoing plasticisation if the safety factor of all the elements it is made of satisfies the requirement $\eta_j \geq 1$. The output of this post-processing is presented in Figure 7, where for the sake of clarity the only optimal solution with six stringers, i.e., the fittest individual with $x_1 = 6$, is shown. The individual is characterised by four numbers that identify (i) the most critical safety factor among those of the structural elements (η_{crit}), computed according to Equation (3), (ii) the index of the stringers section in the database, (iii) the index of the truss section in the database and (iv) the index of the pedestal section in the database.

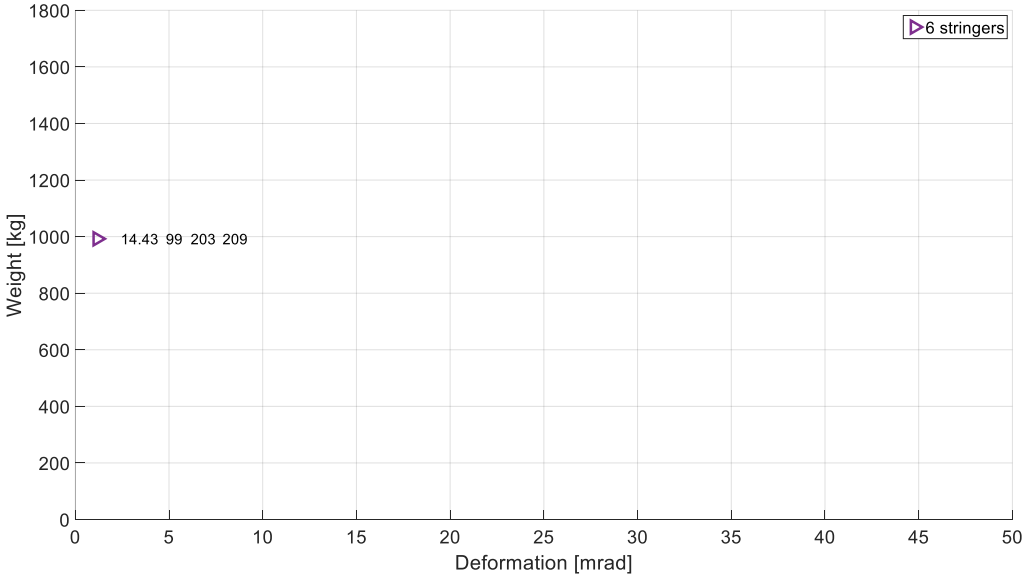

Figure 7. Detailed information of the optimal solution with six stringers.

The individual shown in Figure 7 is characterised by critical safety factor η_{crit} satisfying the requirement $\eta_{crit} \geq 1$ and the corresponding structural solution is determined by hollow rectangular-shaped stringers and hollow circular-shaped truss and pedestal. This solution is physically sound, since circular sections are assigned to those elements undergoing torque, while stringers are described by hollow rectangular sections, which are known to be effective in case no torque is applied.

Moreover, the design variables values, the objective functions values and the most critical safety factor value among those of the structural elements are reported in Table 2 for each of the individuals included in the Pareto front.

Table 2. Properties of the optimal solutions.

x_1	x_2	x_3	x_4	Weight [kg]	Deformation [mrad]	η_{crit}
2	163	116	209	885	1.26	11.55
2	162	116	209	793	1.27	12.22
2	162	115	209	753	1.34	10.14
2	155	115	209	604	1.48	11.20
2	152	115	202	476	3.39	6.48
2	192	152	205	406	3.51	5.47
2	81	108	115	317	5.29	3.59
3	191	155	206	569	2.89	6.15
3	181	142	196	228	20.04	1.74
4	60	83	153	295	20.03	1.44
6	99	203	209	992	1.18	14.43
7	112	16	211	1799	0.73	16.90
7	155	204	212	1357	0.85	14.50
7	155	204	211	1331	0.92	14.50
7	152	204	211	1252	0.94	15.10
7	193	203	211	1175	1.05	13.16
7	149	203	210	1102	1.15	13.76
7	99	203	209	1076	1.16	13.76

As expected, it turns out that the optimal sections for the stringers are mostly identified within the hollow rectangular and square sections in the database, since no torque is applied to this type of element. Moreover, most of the sections of the truss are characterised by hollow rectangular and hollow circular shapes, while the pedestal is almost always characterised by hollow circular sections, which is expected since these two structural elements are subjected to torque. Moreover, it is worth highlighting that (i) no H- and T-shaped sections are identified within the individuals in the Pareto front, (ii) none of the optimal solutions undergoes plasticisation, i.e., $\eta_{crit} \geq 1$, and (iii) some structural solutions admit deformations below the threshold 1mrad, which is a typically pursued value in this field [18].

4. Conclusions

In this work a methodological approach to the multi-objective optimisation of the support structure of heliostats in concentrated solar power plants employing a genetic algorithm has been presented. The proposed approach involves the interaction between the heliostat structural model and the optimiser. The former, which has been presented in Section 2.1, has been implemented in the Excel software package, it is based on the Euler-Bernoulli beam theory and relies on the main assumptions that (i) the mirror stiffness is negligible and (ii) the structural elements, i.e., the stringers, the truss and the pedestal, undergo linear elastic deformations. The latter, which has been described in Section 2.2,

consists of the *gamultiobj* algorithm implemented in the MATLAB® environment, which has been properly modified to work with discrete integer design variables.

The proposed methodological approach has been demonstrated by means of a case study in Section 3. The optimisation has been carried out considering the wind loads from three different inclination angles of the mirror of the heliostat, keeping the wind azimuth angle constant to simulate the most critical scenario. The results of the optimisation are characterised by a Pareto front described by the hyperbolic shape typical of multi-objective optimisation problems and the optimal solutions present physically sound properties. In fact, it has been shown that the stringers are mostly assigned hollow rectangular and square sections, which is expected since no torque is exerted on this type of structural element, while solutions including hollow circular sections for the truss and the pedestal have been identified, which is likely to have been determined due to the torque applied to these two structural elements.

Despite the results of the optimisation process are realistic, the proposed methodology may be further improved to get more accurate results. The structural model employed to evaluate the deformation of the mirror surface may be refined by relaxing the assumptions reported in Section 2.1. For instance, the stiffness of the mirror may be included in the analysis and an analytical theory accounting for the loads not applied to the beam ends in a more accurate way may be implemented. With regards to the optimisation, a finer discretisation of the Pareto Front may be achieved considering a larger number of individuals, even though this would increase the required computational resources. On the other hand, the required computational time may be decreased by implementing the structural model and the optimiser in the same environment to avoid passing the data between the models. Moreover, the evaluation of the plasticisation of the structural elements may be introduced as a constraint to the optimisation process, thus allowing to directly replace those individuals described by solutions in which at least one of the components they are made of undergo plasticisation, even though this would increase the computational effort required to complete the optimisation process.

Funding
The work is part of the Research and Innovation Project “Solargrid: Sistemi sOlari termodinamici e fotovoLtaici con Accumulo peR co-GeneRazIone e flessibilità Di rete ”—cod. ARS01_00532. The project has been jointly funded by the European Union and Italian Research and University Ministry (MIUR) under the Programma Operativo Nazionale “Ricerca e Innovazione” 2014–2020 (PON “R&I” 2014–2020).

Available material
The database including the sections considered in this work is available at https://polimi365-my.sharepoint.com/:b:/g/personal/10421282_polimi_it/ERIFCXbcSCdBozaCY0uKB7kB5c9h-HshXcGHmnE12fSipA?e=vq7l8z.

References
[1] Mancini T R, Gary J A, Kolb G J and Ho C K 2011 *Power Tower Technology Roadmap and cost reduction plan.* (Albuquerque, NM, and Livermore, CA (United States))
[2] Aldaz L, Burisch M, Zaversky F, Sánchez M, Villasante C and Olasolo D 2018 Heliostat structural optimization: A study of wind load effects with CFD-FEM methods *AIP Conf. Proc.* **2033** 210001
[3] Bhargav K R, Gross F and Schramek P 2014 Life Cycle Cost Optimized Heliostat Size for Power Towers *Energy Procedia* **49** 40–9
[4] Blackmon J B 2012 Heliostat size optimization for central receiver solar power plants *Concentrating Solar Power Technology* (Woodhead Publishing) pp 536–76
[5] Pfahl A 2014 Survey of Heliostat Concepts for Cost Reduction *J. Sol. Energy Eng.* **136**
[6] Von Reeken F, Weinrebe G, Keck T and Balz M 2016 Heliostat cost optimization study *AIP*

Conf. Proc. **1734** 20005
[7] Weinrebe G, Von Reeken F, Wöhrbach M, Plaz T, Göcke V and Balz M 2014 Towards Holistic Power Tower System Optimization *Energy Procedia* **49** 1573–81
[8] Todd Griffith D, Moya A C, Ho C K and Hunter P S 2015 Structural Dynamics Testing and Analysis for Design Evaluation and Monitoring of Heliostats *J. Sol. Energy Eng.* **137** 021010
[9] Zang C, Wang Z, Liang W and Wang X 2010 Structural Design and Analysis of the Toroidal Heliostat *J. Sol. Energy Eng.* **132** 041007
[10] Zang C, Wang Z and Liu X 2009 Design and analysis of a novel heliostat structure *1st International Conference on Sustainable Power Generation and Supply, SUPERGEN '09* (Nanjing: IEEE)
[11] Thalange V C, Dalvi V H, Mahajani S M, Panse S V., Joshi J B and Patil R N 2017 Design, optimization and optical performance study of tripod heliostat for solar power tower plant *Energy* **135** 610–24
[12] Belaid A, Filali A, Gama A, Bezza B, Arrif T and Bouakba M 2020 Design optimization of a solar tower power plant heliostat field by considering different heliostat shapes *Int. J. Energy Res.* **44** 11524–41
[13] Timoshenko S 1953 *History of strength of materials* (New York: McGraw-Hill)
[14] Peterka J and Derickson R 1992 *Wind load design methods for ground-based heliostats and parabolic dish collectors* (Albuquerque, NM)
[15] Oppo Srl Tabelle https://www.oppo.it/tabelle/a_elenco_tabelle.html (Accessed 2021-07-21)
[16] MathWorks Find Pareto front of multiple fitness functions using genetic algorithm https://www.mathworks.com/help/gads/gamultiobj.html (Accessed 2021-07-21)
[17] MathWorks gamultiobj Algorithm https://www.mathworks.com/help/gads/gamultiobj-algorithm.html (Accessed 2021-07-21)
[18] Sattler J C, Röger M, Schwarzbözl P, Buck R, Macke A, Raeder C and Göttsche J 2020 Review of heliostat calibration and tracking control methods *Sol. Energy* **207** 110–32